
Reduction of Nitrate Content in Water by the Use of Banana Peels Biochar

Yacouba Zoungranan^{1, *}, Kouassi Kouadio Dobi-Brice², Koutouan Djako Oscar Eric³,
Sombo Anselme Stanislas², Ekou Tchirioua², Ekou Lynda²

¹Department of Mathematics, Physics and Chemistry, University Peleforo Gon Coulibaly, Korhogo, Côte d'Ivoire

²Department of Chemistry, University Nangui Abrogoua, Abidjan, Côte d'Ivoire

³Doctoral School of Science, Technology and Sustainable Agriculture, University Félix Houphoët-Boigny, Abidjan, Côte d'Ivoire

Email address:

zoungranan@gmail.com (Y. Zoungranan), zoungranan@upgc.edu.ci (Y. Zoungranan)

*Corresponding author

To cite this article:

Yacouba Zoungranan, Kouassi Kouadio Dobi-Brice, Koutouan Djako Oscar Eric, Sombo Anselme Stanislas, Ekou Tchirioua, Ekou Lynda. Reduction of Nitrate Content in Water by the Use of Banana Peels Biochar. *American Journal of Physical Chemistry*. Vol. 10, No. 4, 2021, pp. 59-66. doi: 10.11648/j.ajpc.20211004.13

Received: October 9, 2021; **Accepted:** November 1, 2021; **Published:** November 10, 2021

Abstract: The intensification of agricultural, domestic and industrial activities leads to the increasing contamination of groundwater and surface water by nitrates. Indeed, agricultural runoff, septic tank effluents, landfill leachates or wastewater treatment plant effluents contribute to this nitrification, yet drinking water containing high nitrate content can cause health problems. The study examines the improvement of nitrate removal in synthetic water solution by adsorption on banana peel's activated carbon (BPAC). Different effects of physicochemical parameters, such as the optimal contact time of BPAC in solution, the pH of the nitrate solution, the initial concentration of nitrate solution, the BPAC mass, and the temperature were evaluated. The study revealed that BPAC has a low nitrate adsorption capacity under normal laboratory conditions. However, this adsorption capacity of BPAC increases with increasing of temperature and initial content of nitrate, while it decreases with increasing BPAC mass. For a content of 100 mg/L nitrate solution, the maximum adsorption capacity was 0, 687 mg/g for an equilibrium time of 180 min. Nitrate adsorption is optimal in acidic media (pH=3). The application of kinetic models to the experimental data showed that the mechanism of nitrate adsorption on BPAC obeys pseudo-first order kinetics. The Freundlich isotherm perfectly describes the mechanism of nitrate adsorption on BPAC.

Keywords: Adsorption, Nitrates, Activated Carbon, Banana Peels, Models

1. Introduction

According to recent prospective studies [1], out of 180 countries in the world, 87 of them will have water resources of less than 1700 m³ per year and per capita in 2050. The number of countries with absolute water shortages (i.e. with resources of less than 500 m³ per year and per capita) is expected to rise from 25 in 2015 to 45 in 2050. This decrease in water resources is linked in part to population growth and climate change, but above all to pollution phenomena mainly resulting from human activities. Indeed, industrial, agricultural and domestic activities generate numerous pollutants, including nitrates (NO₃⁻) which are likely to degrade the quality of groundwater and surface water [2, 3].

The excess of NO₃⁻ in surface waters leads to the phenomenon of eutrophication [4, 5] which is a phenomenon related to a surplus of nutrients. In addition, too high concentrations of nitrates in drinking water can cause many human health problems. Excessive nitrates in infants can cause pathologies such as methemoglobinemia [6]. In adults, excess nitrate can lead to gastric cancer, colon cancer [7] and other cancers related to the formation of nitrosamines [8]. These human health problems caused by nitrate have led the World Health Organization (WHO) [9], to set the maximum level of nitrate in drinking water at 50 mg/L, while this threshold is set at 10 mg/L by the US Environmental Protection Agency (US EPA) [10]. The reduction of nitrate contents in drinking water has therefore become a huge

health and environmental challenge [11].

Numerous methods have been developed for the removal of nitrate from contaminated water. Among them, coagulation-coagulation [12], nanofiltration [13], reverse osmosis [14], electrochemistry [15] and many others. However, these methods, although effective, remain costly, difficult to implement and sometimes inaccessible to developing countries. To overcome these difficulties, the scientific community is increasingly interested in other methods such as the adsorption, which is just as effective and less expensive [7, 16]. Several adsorption studies on activated carbon have been carried out. Among these we can mention adsorption on activated carbon based on rice husk [17]; based on pine cones [18] and based on tree branches [8]. It is in this perspective that we use in the present study an activated carbon based on plantain peels in order to reduce by adsorption, the nitrate content in water. The influence of some physico-chemical parameters on the adsorption was evaluated throughout this document. Some components, such as multi-leveled equations, graphics, and tables are not prescribed, although the various table text styles are provided. The formatter will need to create these components, incorporating the applicable criteria that follow.

2. Material and Methods

2.1. Plant Material

Bananas were harvested from a plantation located 5 km east of the town of Bonoua (Côte d'Ivoire). The banana samples were placed in vegetable fiber bags and immediately transported to the laboratory. The bananas underwent a washing and peeling process to obtain clean banana peels. The banana peels washed with distilled water were dried in an oven (Memmert BM300, Schwabach, Germany) at 105°C for 48 h.



Figure 1. Dried banana peels.

2.2. Process for Obtaining the BPAC

The dried banana peel samples were placed in porcelain crucibles and then calcined at 550°C using a muffle furnace (Nabertherm GmbH, Bremen, Germany) for 1 h. The carbonisate was ground using a porcelain pestle and mortar and the resulting charcoal powder was sieved using a sieve (Saulas, Paris, France) to select a particle size of 100 µm. The banana peel charcoal was then subjected to a physical activation process. For this, 100 g of charcoal powder was

mixed with 20 mL of distilled water. The mixture was placed in the muffle furnace at 650°C for 1 h under a gradient of 5°/min. After cooling, the powder was washed with distilled water on a Buchner to neutral pH. The powder is oven dried for 24 h at 105°C to obtain the BPAC.

2.2.1. CAPB Moisture and Ash Content

The moisture content indicates the water content in the BPAC. A porcelain crucible containing 2 g of BPAC (m_1) is placed in the oven at 105°C for 24 h for drying. The mass of the dry sample is noted m_2 . The sample is then calcined at 950°C in a muffle furnace for 1 h and the mass of residue obtained is noted m_3 . The moisture content H (%) and the fire mass loss or ash content C (%) of the CAPB are given by the following relations:

$$H(\%) = \frac{m_1 - m_2}{m_1} \times 100 \quad (1)$$

$$C(\%) = \frac{m_2 - m_3}{m_2} \times 100 \quad (2)$$

2.2.2. CAPB Density

An empty 100 mL test tube is weighed and its mass is noted as M_1 . The test tube is then filled with CAPB to jauge mark and the mass of the whole is noted M_2 . The density is determined from relation 3.

$$d = \frac{M_2 - M_1}{100} \quad (3)$$

2.2.3. CAPB's pH of Zero Charge

The pH values of 9 solutions of 0.1 M sodium chloride were adjusted by adding HCl (0.1 M) or NaOH (0.1 M) in order to have initial pH values (pHi) ranging from 2 and 10. The pH values are measured with a pH meter (Hanna HI 9813-5, Bucharest, Romania). In each beaker a mass of 1 g of CAPB is placed and the whole kept under stirring for 48 hours. The final pH values (pHf) of the solutions after filtration are measured. The plot $\text{pHf} = f(\text{pHi})$ intersects the line ($\text{pHi} = \text{pHf}$) at the point of zero charge noted pHzc .

2.3. Batch Adsorption Studies

2.3.1. Method of Operation

For all tests, a stock of potassium nitrate solution of concentration C_0 (100 mg/L) was carefully prepared. The desired C_i concentrations will be obtained by diluting this stock.

In each experiment, a mass m of 1 g of CAPB is placed in a 250 mL beaker containing 50 mL (V_i) of potassium nitrate solution of concentration C_i . The mixture is stirred at 300 rpm for a given time t_f , using a vibrating shaker (Heidolph Vibramax 100, Germany). After stirring, the mixture is filtered under gravity to obtain a final volume V_f . The filtrate is centrifuged at 7000 rpm for 5 minutes. 5 mL of the supernatant is taken and diluted 10 times. Volume of 10 mL of diluted solution is placed in a jar and 0.5 mL of azide and

0.2 mL of acetic acid are successively added. The jar is heated to 95°C in a water bath until total evaporation of the contents. After cooling, 1mL of 1% sodium salicylate solution is added and evaporated in the water bath. A white solid residue appears. The solid residue is cooled and 1 mL of 1 M sulfuric acid solution is added. After 15 minutes, 15 mL of distilled water and 10 mL of sodium hydroxide solution are added. The mixture turns yellow indicating the complexation of the nitrates. The optical density of the complex is read at 415 nm with a UV/visible spectrophotometer (WFJ-752, China). The different nitrate concentration was determined from the calibration curve established with potassium nitrate. The amounts of nitrate adsorbed on the BPAC were determined using the following formula [19]:

$$q = \frac{C_i V_i - C_f V_f}{m} \quad (4)$$

2.3.2. Influence of Physicochemical Parameters

The contact time study was performed by placing 0.5 g of BPAC in solutions of initial concentration C_i equal to 100 mg/L. The stirring times were 15min, 30 min, 60 min, 90 min 120 min, 150 min, 180 min, 210 min and 240 min.

For the effect of BPAC mass, masses of 0.5g, 1g, 1.5g, 2g, 2.5g and 3g of BPAC were contacted with the nitrate solutions of initial concentration C_i equal to 100 mg/L. The duration of agitation was 3 hours.

The influence of the initial concentration was done by diluting the stock solution to obtain the concentrations 20 mg/L, 30 mg/L, 40 mg/L, 50 mg/L, 60 mg/L, 70 mg/L, 80 mg/L, 90 mg/L. The stirring time is set to 3 hours.

For the influence of the pH of the initial solution, the initial concentration of each solution is set to 100 mg/L and the pH values are adjusted by adding NaOH (1M) or HCl (1M) so as to have pH values: 2, 3, 4, 5, 6, 7, 8, 9 and 10. The duration of agitation was 3 hours.

Finally, for the evaluation of the influence of temperature, the initial concentration of the solutions is also 100 mg/L and the stirring time is 3 hours. The temperatures were adjusted to 0°C; 10°C; 20°C; 40°C and 60°C

2.4. Batch Study's Results Modeling

2.4.1. Pseudo-first Order Kinetic Model

Lagergren's pseudo-first order model [20] is the first rate equation established for the description of adsorption kinetics in a liquid-solid system. This model is based on the assumption that the sorption rate q decreases linearly with the adsorption capacity [21].

$$\ln(q_e - q) = \ln(q_e) - k_1 t \quad (5)$$

With:

- k_1 : rate constant for pseudo first order kinetics (min^{-1}).
- q : adsorption capacity at time t (mg/g),
- q_e : adsorption capacity at equilibrium (mg/g),
- t : duration of the adsorption process.

The kinetic parameters k_1 and q_e of the model, are determined from the graph

$$\ln(q_e - q) = f(t) \quad (6)$$

2.4.2. Pseudo-second Order Kinetic Model

The pseudo-second order model [22] assumes that the reaction rate depends on the amount q adsorbed at time t and the amount q_e adsorbed at equilibrium. The model also considers that the limiting step is the interaction between the adsorbent and the solute [23].

The equation of this model is:

$$\frac{t}{q} = \frac{1}{k_2 q_e} + \frac{t}{q_e} \quad (7)$$

k_2 : pseudo second order rate constant ($\text{g} \cdot \text{mg}^{-1} \cdot \text{min}^{-1}$),

q : adsorption capacity at time t (mg/g),

q_e : adsorption capacity at equilibrium (mg/g).

The kinetic parameters of the model are determined from the graph:

$$\frac{t}{q} = g(t) \quad (8)$$

2.4.3. The Langmuir Isotherm

The Langmuir isotherm [24] is derived from a kinetic mechanism which permit to determine the maximum adsorption quantity and the equilibrium adsorption constant. It assumes a monolayer adsorption in which the adsorbent and the adsorbate are in dynamic equilibrium.

The linearized Langmuir isotherm is translated by the following equation:

$$\frac{C_e}{q_e} = \frac{1}{q_{\max} K_L} + \frac{C_e}{q_{\max}} \quad (9)$$

With:

q_e : amount of solute adsorbed per gram of adsorbent (mg/g) at equilibrium,

q_{\max} : maximum quantity of adsorption (mg/g),

C_e : concentration of the solute (mg/L) in the solution at equilibrium,

K_L : Langmuir constant (L/g).

The parameters of Langmuir's isotherm are determined from the graph:

$$\frac{C_e}{q_e} = h(t) \quad (10)$$

2.4.4. The Freundlich Isotherm

The Freundlich isotherm [25] is an empirical equation that assumes that adsorption occurs on a heterogeneous surface and is not limited to monolayer formation so that multilayer adsorption is possible. The Freundlich model also assumes that adsorption is reversible and that the amount adsorbed increases indefinitely with an increase in adsorbate concentration. The Freundlich model is given by the

following relationship:

$$\ln(K_D) = j(t) \tag{18}$$

$$\ln(q_e) = \ln(K_F) + \frac{1}{n} \ln(C_e) \tag{11}$$

With:

q_e : amount of solute adsorbed per gram of adsorbent (mg/g) at equilibrium,

C_e : concentration of the solute (mg/L) in the solution at equilibrium,

K_F : Freundlich constant (L/g)

n : empirical parameter depending on the heterogeneity of the matrix.

The adsorption is said to be irreversible for ($1/n = 0$), favorable for ($0 < 1/n < 1$) and unfavorable for ($1/n > 1$) [26]. The parameters of the Freundlich isotherm are determined from the graph:

$$\ln(q_e) = i(t) \tag{12}$$

2.4.5. Paramètres Thermodynamiques

In the adsorption process, the adsorbent (A) interacts with the adsorbate (B) to give AB [27]. Thermodynamic quantities such as the standard Gibbs free energy (ΔG°), standard enthalpy (ΔH°) and standard entropy (ΔS°) are used to evaluate the spontaneity, thermal character and nature of the adsorption reaction [28].

The Gibbs free energy change (ΔG) tends to zero, at chemical equilibrium [29] which leads to the following expression:

$$\Delta G = \Delta G^\circ + RT \ln(K_e) = 0 \tag{13}$$

With

R: universal constant of perfect gases,

T: temperature

K_e : thermodynamic equilibrium constant.

The thermodynamic equilibrium constant K_e is equal to the distribution coefficient K_D at the adsorption equilibrium [30].

$$K_D = \frac{q_e}{C_e} \tag{14}$$

According to the Ellingham approximation:

$$\Delta G^\circ = \Delta H^\circ - T\Delta S^\circ \tag{15}$$

We thus obtain the following relationship:

$$\ln(K_D) = -\frac{\Delta H^\circ}{RT} + \frac{\Delta S^\circ}{R} \tag{16}$$

And

$$\Delta G^\circ = -RT \ln(K_D) \tag{17}$$

The values of ΔH° and ΔS° are determined from the plot of:

3. Results and Discussion

3.1. Brief Description of the BPAC

The resulting banana peel biochar has the appearance shown in Figure 2. The characteristics such as moisture content, fire mass loss, density and pH of the BPAC are presented in Table 1.



Figure 2. CAPB photograph.

Table 1. Some characteristics of BPAC.

BPAC	
Moisture content H (%)	9.5
Fire mass loss C (%)	96
Density (d)	0.25
pH _{zc}	6.2

3.2. Adsorption Kinetics

3.2.1. Adsorption Equilibrium Time

The results of the contact time study are shown in Figure 3.

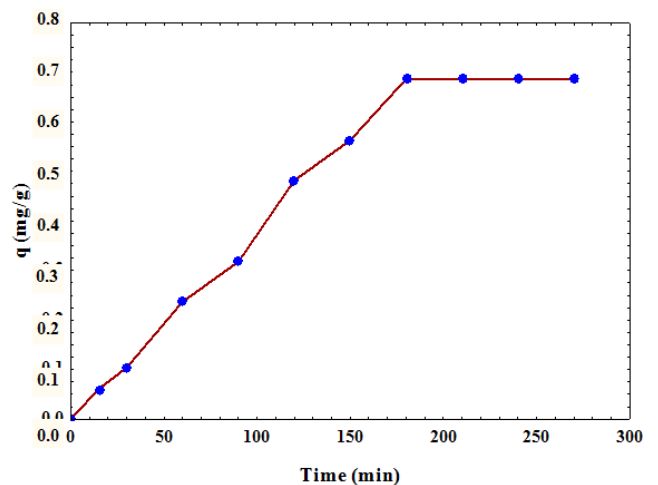


Figure 3. Amount of nitrate adsorbed over time, in mg/g BPAC.

The analysis of figure 3, shows that the amount of nitrate removed increases with time until reaching a plateau after 180 min. This plateau reflects the chemical equilibrium of

adsorption and corresponds to the occupation of the majority of the BPAC sites by nitrate ions [31]. At chemical equilibrium, the maximum amount of nitrate adsorbed by BPAC is $q_{e, \max} = 0.687 \text{ mg/g}$. Beyond the adsorption equilibrium, there is a decreasing availability of the many remaining active sites on the BPAC surface. Therefore, the amount of adsorbed nitrate becomes constant and of insignificant variation over time.

3.2.2. Pseudo-order of the Adsorption Reaction

The pseudo order of reaction obtained from the experimental data, provides insight into the mechanism of adsorption process [7, 32, 21]. The application of experimental data to the pseudo-first order and pseudo-second order models, are given by Figure 4 and Figure 5. The results of the calculation of the kinetic parameters are presented in Table 2.

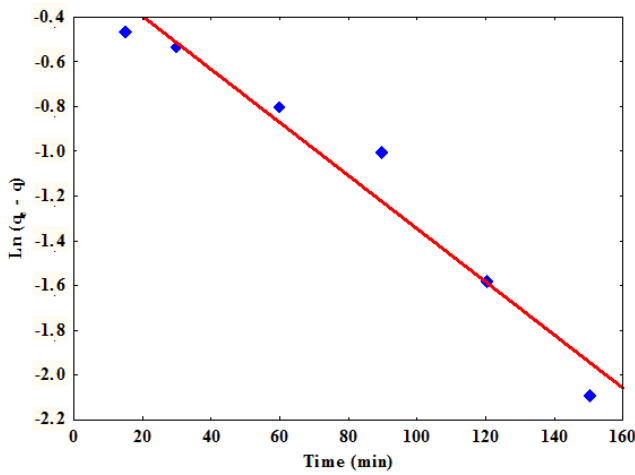


Figure 4. Result of the pseudo-first order model.

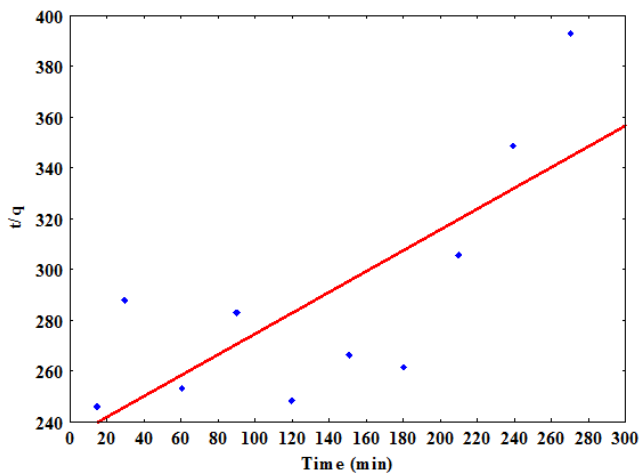


Figure 5. Result of the pseudo-second order model.

Table 2. Kinetic parameters of pseudo-first and pseudo-second order models ($q_{e, \exp}$ (mg/g), $q_{e, \text{the}}$ (mg/g), k_1 (min⁻¹) and k_2 (g/mg.min).

Pseudo-first order				Pseudo-second order			
$q_{e, \text{the}}$	$q_{e, \exp}$	k_1	R^2	$q_{e, \text{the}}$	$q_{e, \exp}$	k_2	R^2
0.852	0.687	0.012	0.95	2.44	0.687	$7.21 \cdot 10^{-3}$	0.57

The analysis of Table 2 shows that the coefficient of determination $R^2 = 0.95 > 0.9$ for the pseudo-first order kinetic model is higher than that of the pseudo-second order (0.57). In addition, the theoretical (q_e) value ($q_{e, \text{the}}$) calculated from the pseudo-first order model shows good agreement with the experimental (q_e) value ($q_{e, \exp}$) compared to the pseudo-second order. The adsorption of nitrate on BPAC thus follows pseudo-first order kinetics. This suggests that the adsorption of nitrate on BPAC follows a physisorption mechanism. Dong et al [33] on the other hand showed in their study on the adsorption of nitrate on modified granular activated carbon that the kinetic model obeyed a pseudo-second order reflecting a chemical adsorption. It is therefore possible that the modification of the surface of the adsorbent can modify the nature of the adsorption.

3.3. BPAC Mass Effect

The results of the influence of the mass of BPAC on its ability to adsorb nitrates in a constant volume are shown in Figure 6.

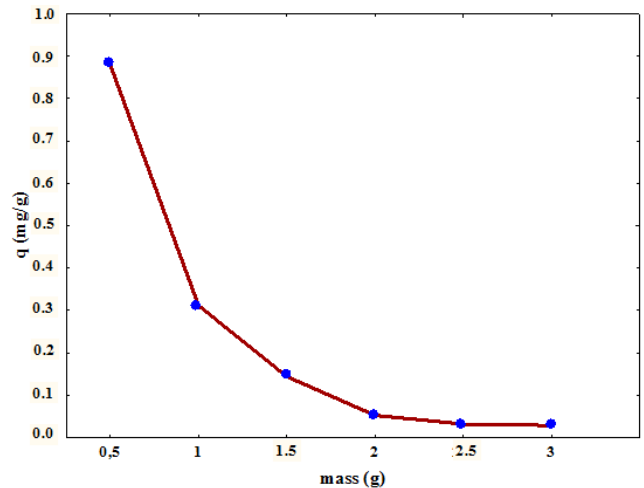


Figure 6. Amount of nitrate adsorbed as a function of BPAC mass, in mg/g BPAC.

The amount of nitrate adsorbed decreases with increasing BPAC mass, this may be explained by a greater availability of active sites of BPAC in the low proportions. The decrease in removal capacity with increasing BPAC mass could be attributed to the decrease in the total surface area of BPAC accessible by the solute [34]. The results of this study are in agreement with those obtained by Mazarji et al [7] in their study of nitrate removal from aqueous solution using modified granular activated carbon. These authors showed in their work that the amount of nitrate adsorbed decreased from 11 to 3.33 mg/g with increasing adsorbent mass.

3.4. Effect of pH

The result of the influence of the pH of the initial solution on the adsorption of nitrates by CAPB is shown in figure 7.

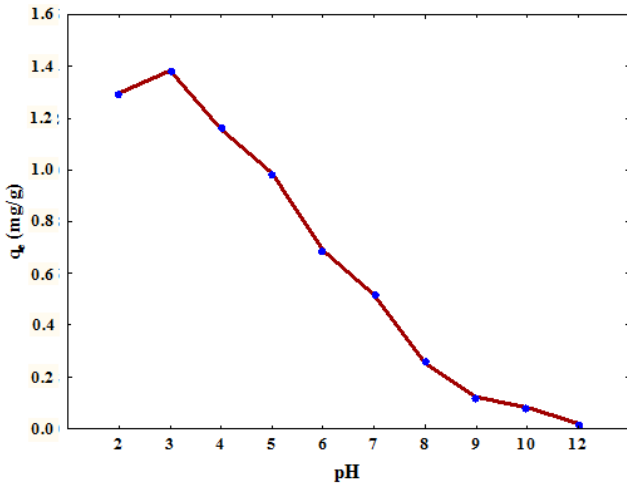


Figure 7. Amount of nitrate adsorbed (mg/g BPAC) as a function of solution's initial pH.

The BPAC's pH value of zero charge point is 6.2 (Table 1). This value corresponds to the pH value for which the resultant of the positive and negative charges on the surface is zero. This means that for pH values < 6.2 the BPAC surface is positively charged and for pH values > 6.2 it is negatively charged. The amount of nitrate adsorbed is highest at pH 3, above this value the increase in pH does not promote nitrate adsorption. The better amounts of adsorbed nitrate with acidic pH values could be explained by the intensification of the attractive Van der Waals forces between the nitrate ions and at the positive surface of BPAC. The low amount of nitrate adsorbed at pH < 3, may be related to a competition phenomenon between Cl⁻ ions (from HCl addition) and nitrate ions. For pH > 3 values, the drop in adsorbed amounts is related to the increase of negative sites on the BPAC surface. There is indeed, a phenomenon of electrostatic repulsion. Similar results were also reported by Mazarji et al [38]. These authors showed in a study of nitrate removal using modified granular activated carbon, that the best rate of nitrate removal was obtained in an acidic medium at pH = 5.

3.5. Adsorption Isotherms

The study of the concentration effect showed that the

amount of nitrate removed by BPAC increased with the initial concentration of nitrate in solution. This result could be explained by the accelerated diffusion of nitrate ions on BPAC due to the increase in the concentration gradient [35]. The experimental data from the study were applied to the Freundlich and Langmuir models. The results are given in figures 8 and 9.

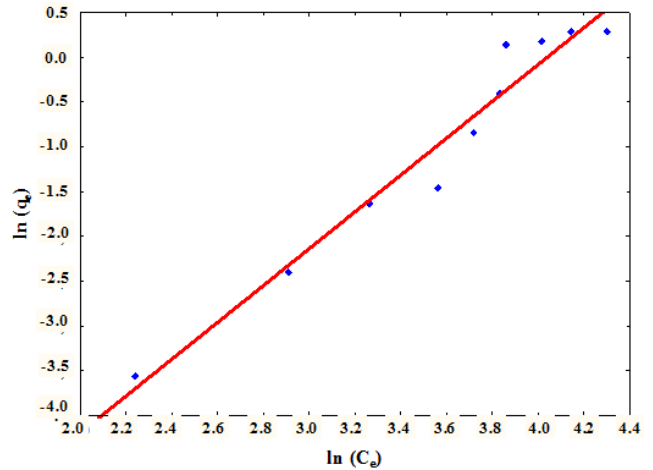


Figure 8. Freundlich isotherm of nitrate adsorption.

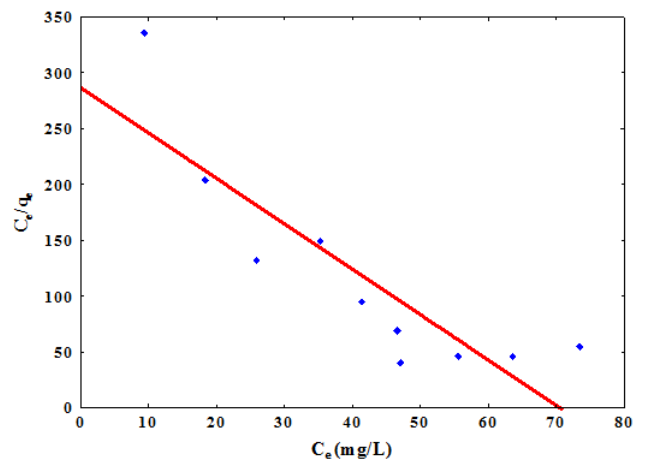


Figure 9. Langmuir isotherm of nitrate adsorption.

The results of parameters's calculation are shown in the table below.

Table 3. Langmuir's and Freundlich's models parameters in the adsorption of nitrate on BPAC.

Langmuir			Freundlich		
q _{max} (mg/g)	K _L (L/mg)	R ²	1/n	K _F (L/g)	R ²
-0.2456	-0.0142	0.75	0.486	2.459.10 ⁻⁴	0.96

The value of the constant 1/n of the Freundlich isotherm is 0.486. This result means that the adsorption of nitrate on BPAC is favorable. The comparison of the coefficients of determination shows that the nitrate adsorption is better described by the Freundlich model. On the other hand, the results of the work of Heba et al [36] on the adsorption of aqueous nitrate ions by activated carbon based on solid olive waste using ZnCl₂ revealed good agreement with the

Langmuir model. As for Reza et al [37], they showed in the kinetic, isothermal and thermodynamic study of nitrate adsorption from aqueous solution using modified rice husks that Freundlich, Langmuir and Dubinin-Radushkevich models all agreed well with the experimental results.

3.6. Thermodynamic Aspects

The influence of temperature on nitrate adsorption by

BPAC was evaluated through the determination of the standard thermodynamic quantities ΔH° , ΔS° and ΔG° . These quantities are determined by applying the experimental results of the amounts of nitrate adsorbed as a function of temperature to equations (Eq. 16) and (Eq. 17). The thermodynamic quantities obtained are recorded in Table 4.

Table 4. Standard thermodynamic quantities in nitrate adsorption by BPAC.

T (K)	ΔG° (kJ/mol)	ΔH° (kJ/mol)	ΔS° (J/mol)
293	-6013.01127		
303	-4181.94703		
313	-1962.94982	-50.463	-152.772
323	-1020.09436		
333	-50.4918919		

The negative value of ΔH° indicates that the nitrate adsorption reaction by BPAC is exothermic. It is promoted by lowering the temperature. This implies that temperature allows for increased mobility of nitrate ions but could cause crowding for access to adsorption sites on the BPAC surface. Other work made by different authors [37, 39] have also mentioned the exothermic nature of nitrate adsorption. The negative values of the standard Gibbs free energy (ΔG°) obtained at different temperatures confirm the spontaneous nature of the nitrate adsorption process by BPAC. The low values of ΔG° ($<10 \text{ kJ}\cdot\text{mol}^{-1}$) [21] obtained, allows to confirm the physical process in nitrates adsorption on BPAC. The standard entropy ΔS° is negative over the temperature range of the study, this reflects a decrease in the degree of freedom of nitrates and a decrease in disorder at the BPAC/nitrate interface [40]. This decrease shows that the transition state is more ordered than the initial state. It also reveals an organized distribution of nitrate ions at the BPAC adsorption sites [41].

4. Conclusion

The study aims to valorize agricultural waste such as banana peels by using it as an adsorbent to reduce nitrate content in water. The study showed that banana peel activated carbon can adsorb nitrates and provided removal in small amounts. Parameters such as contact time, solution pH, adsorbent mass, temperature and initial nitrate concentration affect the adsorption capacity of the activated biochar. Maximum adsorption is obtained for an equilibrium time of 180 min. The adsorption process of nitrate by banana peels's activated carbon, perfectly obeys the pseudo-first order kinetics and the equilibrium follows the Freundlich isotherm. The increase in mass resulted in a decrease in the amount of nitrate from 0.886 mg/g to 0.027 mg/g for a mass change from 0.5 g to 3g. Nitrate adsorption is optimal at pH = 3 and is enhanced by a decrease in temperature.

Acknowledgements

The authors would like to thank the Department of Chemistry of the University Nangui Abrogoua (RCI) and specifically the Laboratory of Thermodynamics and

Environmental Physicochemistry, for the facilities made available to them to conduct this research work.

References

- [1] Baggio, G., Qadir, M., & Smakhtin, V. (2021). Freshwater availability status across countries for human and ecosystem needs. *Science of The Total Environment*, 792, 148230.
- [2] Murgulet, D., & Tick, G. R. (2013). Understanding the sources and fate of nitrate in a highly developed aquifer system. *Journal of Contaminant Hydrology*, 155, 69–81.
- [3] Lockhart, K. M., King, A. M., & Harter, T. (2013). Identifying sources of groundwater nitrate contamination in a large alluvial groundwater basin with highly diversified intensive agricultural production. *Journal of Contaminant Hydrology*, 151, 140–154.
- [4] Yoshino, H., Tokumura, M., & Kawase, Y. (2014). Simultaneous removal of nitrate, hydrogen peroxide and phosphate in semiconductor acidic wastewater by zero-valent iron. *Journal of Environmental Science and Health - Part A Toxic/Hazardous Substances and Environmental Engineering*, 49 (9), 998–1006.
- [5] Chen, S., Wu, W., Hu, K., & Li, W. (2010). The effects of land use change and irrigation water resource on nitrate contamination in shallow groundwater at county scale. *Ecological Complexity*, 7 (2), 131–138.
- [6] Wu, Y., Wang, Y., Wang, J., Xu, S., Yu, L., Philippe, C., & Wintgens, T. (2016). Nitrate removal from water by new polymeric adsorbent modified with amino and quaternary ammonium groups: Batch and column adsorption study. *Journal of the Taiwan Institute of Chemical Engineers*, 66, 191–199.
- [7] Mazarji, M., Aminzadeh, B., Baghdadi, M., & Bhatnagar, A. (2017a). Removal of nitrate from aqueous solution using modified granular activated carbon. *Journal of Molecular Liquids*, 233, 139–148.
- [8] Manjunath, S. V., & Kumar, M. (2018). Evaluation of single-component and multi-component adsorption of metronidazole, phosphate and nitrate on activated carbon from *Prosopis juliflora*. *Chemical Engineering Journal*, 346, 525–534.
- [9] WHO, W. H. O. (2017). *Guidelines for Drinking-water Quality fourth edition incorporating the first addendum*. New York, USA.
- [10] USEPA, U. E. P. A. (2018). *2018 Edition of the Drinking Water Standards and Health Advisories Tables (EPA 822-F-18-001)*.
- [11] Ao, L., Xia, F., Ren, Y., Xu, J., Shi, D., Zhang, S., ... He, Q. (2019). Enhanced nitrate removal by micro-electrolysis using Fe0 and surfactant modified activated carbon. *Chemical Engineering Journal*, 357, 180–187.
- [12] Berkani, I., Belkacem, M., Trari, M., & Lapique, F. (2019). Journal of Environmental Chemical Engineering Assessment of electrocoagulation based on nitrate removal, for treating and recycling the Saharan groundwater desalination reverse osmosis concentrate for a sustainable management of Albien resource. *Journal of Environmental Chemical Engineering*, 7 (2), 102951.

- [13] Epsztein, R., Nir, O., Lahav, O., & Green, M. (2015). Selective nitrate removal from groundwater using a hybrid nanofiltration-reverse osmosis filtration scheme. *Chemical Engineering Journal*, 279, 372–378.
- [14] Schoeman, J. J., & Steyn, A. (2003). Nitrate removal with reverse osmosis in a rural area in South Africa. *Desalination*, 155 (1), 15–26.
- [15] Ma, X., Li, M., Feng, C., & He, Z. (2020). Electrochemical nitrate removal with simultaneous magnesium recovery from a mimicked RO brine assisted by in situ chloride ions. *Journal of Hazardous Materials*, 388, 122085.
- [16] Dobi-brice, K. K., Lynda, E., Zounggran, Y., & Tchirioua, E. (2020). Theoretical Characteristics of Deactivated Lichens Fixed Bed Column for the Crystal Violet and. *American Journal of Water Resources*, 8 (2), 69–77.
- [17] Satayeva, A. R., Howell, C. A., Korobeinyk, A. V., Jandosov, J., Inglezakis, V. J., Mansurov, Z. A., & Mikhalovsky, S. V. (2018). Investigation of rice husk derived activated carbon for removal of nitrate contamination from water. *Science of the Total Environment*, 630, 1237–1245.
- [18] Nunell, G. V., Fernandez, M. E., Bonelli, P. R., & Cukierman, A. L. (2015). Nitrate uptake improvement by modified activated carbons developed from two species of pine cones. *Journal of Colloid and Interface Science*, 440, 102–108.
- [19] Jin, X., Jiang, M., Shan, X., Pei, Z., & Chen, Z. (2008). Adsorption of methylene blue and orange II onto unmodified and surfactant-modified zeolite. *Journal of Colloid and Interface Science*, 328 (2), 243–247.
- [20] Lagergren, S., Svenska, B. K., & Handl, V. (1996). "Removal of Arsenite and Arsenate Ions from Aqueous Solution by Basic Yttrium Carbonate" (as cited by Wasey et al.). *Water Research*, 30 (5), 1143 – 1148.
- [21] Divband Hafshejani, L., Hooshmand, A., Naseri, A. A., Mohammadi, A. S., Abbasi, F., & Bhatnagar, A. (2016). Removal of nitrate from aqueous solution by modified sugarcane bagasse biochar. *Ecological Engineering*, 95, 101–111.
- [22] Ho, Y., & McKay, G. (1999). Pseudo-second order model for sorption processes. *Process Biochemistry*, 34 (5), 451–465.
- [23] Reghioua, A., Barkat, D., Jawad, A. H., Abdulhameed, A. S., & Khan, M. R. (2021). Synthesis of Schiff's base magnetic crosslinked chitosan-glyoxal/ZnO/Fe₃O₄ nanoparticles for enhanced adsorption of organic dye: Modeling and mechanism study. *Sustainable Chemistry and Pharmacy*, 20, 100379.
- [24] Langmuir, I. (1918). The adsorption of gases on plane surfaces of glass, mica and platinum. *Journal of the American Chemical Society*, 40 (9), 1361–1403.
- [25] Freundlich, H. M. F. (1906). Über die adsorption in losungen. *Zeitschrift Fur Physikalische Chemie-Leipzig*, 57, 385–470.
- [26] Kono, H., & Kusumoto, R. (2015). Removal of anionic dyes in aqueous solution by flocculation with cellulose ampholytes. *Journal of Water Process Engineering*, 7, 83–93.
- [27] Ruthven, D. M. (1984). *Principles of adsorption and adsorption processes*. (Wiley). New York.
- [28] Crini, G., & Badot, P.-M. (2008). Application of chitosan, a natural aminopolysaccharide, for dye removal from aqueous solutions by adsorption processes using batch studies: A review of recent literature. *Progress in Polymer Science*, 33 (4), 399–447.
- [29] Zhang, D. Y. C. (2014). Adsorption kinetics, isotherm and thermodynamics studies of flavones from *Vaccinium bracteatum* Thunb leaves on NKA-2 resin. *Chem Eng J*, 254, 579–585.
- [30] Elmoubarki, R., Mahjoubi, F. Z., Tounsadi, H., Moustadraf, J., Abdennouri, M., Zouhri, A., ... Barka, N. (2015). Adsorption of textile dyes on raw and decanted Moroccan clays: Kinetics, equilibrium and thermodynamics. *Water Resources and Industry*, 9, 16–29.
- [31] Shukla, A., Zhang, Y.-H., Dubey, P., Margrave, J., & Shukla, S. S. (2002). The role of sawdust in the removal of unwanted materials from water. *Journal of Hazardous Materials*, 95 (1–2), 137–152.
- [32] Stavrinou, A., Aggelopoulos, C. A., & Tsakiroglou, C. D. (2018). Exploring the adsorption mechanisms of cationic and anionic dyes onto agricultural waste peels of banana, cucumber and potato: Adsorption kinetics and equilibrium isotherms as a tool. *Journal of Environmental Chemical Engineering*, 6 (6), 6958–6970.
- [33] Cho, D. W., Chon, C. M., Kim, Y., Jeon, B. H., Schwartz, F. W., Lee, E. S., & Song, H. (2011). Adsorption of nitrate and Cr(VI) by cationic polymer-modified granular activated carbon. *Chemical Engineering Journal*, 175 (1), 298–305.
- [34] Li, Y., Du, Q., Liu, T., Sun, J., Jiao, Y., Xia, Y., ... Wu, D. (2012). Equilibrium, kinetic and thermodynamic studies on the adsorption of phenol onto graphene. *Materials Research Bulletin*, 47 (8), 1898–1904.
- [35] Dobi-brice, K. K., Lynda, E., Zounggran, Y., Sévariste, K. K., & Tchirioua, E. (2020). Use of deactivated lichens for the adsorption of two toxic dyes: crystal violet and methyl red. *Asian Journal of Science And Technology*, 11 (4), 10911–10919.
- [36] Nassar, H., Zyoud, A., El-Hamouz, A., Tanbour, R., Halayqa, N., & Hilal, H. S. (2020). Aqueous nitrate ion adsorption/desorption by olive solid waste-based carbon activated using ZnCl₂. *Sustainable Chemistry and Pharmacy*, 18, 100335.
- [37] Katal, R., Baei, M. S., Rahmati, H. T., & Esfandian, H. (2012). Kinetic, isotherm and thermodynamic study of nitrate adsorption from aqueous solution using modified rice husk. *Journal of Industrial and Engineering Chemistry*, 18 (1), 295–302.
- [38] Mazarji, M., Aminzadeh, B., Baghdadi, M., & Bhatnagar, A. (2017b). Removal of nitrate from aqueous solution using modified granular activated carbon. *Journal of Molecular Liquids*, 233, 139–148.
- [39] Abu, A., & Abdullah, N. (2020). Sorption and thermodynamic study of nitrate removal by using Amberlite IRA 900 (AI900) resin. *Materials Today: Proceedings*, 41, 102–108.
- [40] Dobi-brice, K. K., Lynda, E., Tchirioua, E., & Zounggran, Y. (2018). Biosorption of Methylene Blue and Orange II on deactivated lichen *Parmotrema dilatatum*: Modeling and kinetic studies. *Australian Journal of Basic and Applied Sciences*, 12 (12), 83–89.
- [41] Shoukat, S., Bhatti, H. N., Iqbal, M., & Noreen, S. (2017). Mango stone biocomposite preparation and application for crystal violet adsorption: A mechanistic study. *Microporous and Mesoporous Materials*, 239, 180–189.